Macrocycles

International Edition: DOI: 10.1002/anie.201802159
German Edition: DOI: 10.1002/ange.201802159

Frustrated Helicity: Joining the Diverging Ends of a Stable Aromatic Amide Helix to Form a Fluxional Macrocycle

Ko Urushibara, Yann Ferrand, Zhiwei Liu, Hyuma Masu, Vojislava Pophristic, Aya Tanatani, and Ivan Huc**

Abstract: *Macrocyclization of a stable two-turn helical aromatic pentamide, that is, an object with diverging ends that are not prone to cyclization, was made possible by the transient introduction of disruptors of helicity in the form of acid-labile dimethoxybenzyl tertiary amide substituents. After removal of the helicity disruptors, NMR, X-ray crystallography, and computational studies show that the macrocycle possesses a strained structure that tries to gain as high a helical content as possible despite being cyclic. Two points of disruption of helicity remain, in particular a cis amide bond. This point of disruption of helicity can propagate along the cycle in a fluxional manner according to defined trajectories to produce ten degenerate conformations.*

By definition, the two ends of a molecular helix diverge and are not preorganized to undergo macrocyclization. An exception is when helix is much longer than its persistence length and can bend so that its ends meet, as in circular DNA structures.[1] Macrocyclization of a helix entails some sort of strain. Strained structures are of general interest because they are often associated with unusual conformations and chemical reactivity as illustrated by the properties of bridged[2] and hindered[3] tertiary amides, and by the low occurrence of *cis* secondary amides in proteins.[4] Herein, we report on the conformational frustration of an aromatic pentamide sequence, which is normally prone to form a very stable two-turn helix,[5] upon the formation of a homomeric macrocycle. Macrocyclization was made possible by the temporary introduction of disruptors of helicity in the form of acid-labile 2,4-dimethoxybenzyl (DMB) tertiary amides. We find that the strained macrocycle combines segments that fulfill helix-like conformations and local points of disruption of helicity, including a *cis* secondary amide. The outcome is a loss of symmetry of the macrocycle, which becomes fluxional as the points of disruption of helicity circulate along defined conformational pathways. This approach may serve as an entry to novel entities with complex conformations and conformational dynamics, such as the infinite propagation of defects along long circular molecules.

Some aromatic oligoamide foldamers have been shown to adopt remarkably stable helically folded conformations.[6] For example, octaamide helices of 8-amino-2-quinolinecarboxylic acid (termed Q in the following) remain folded at 120 °C in DMSO, and their interconversion between *P*- and *M*-helical forms is kinetically inert in water.[5,7] This stability arises in part from forces associated with intramolecular aromatic stacking, but an essential contribution lies in local conformational preferences, for example, bifurcated hydrogen bonds and electrostatic repulsions, that set the relative orientations of contiguous amide and aryl units and impart curvature (Figure 1 a).

Aromatic amide sequences that are too short to be helical can adopt crescent shapes.[8] When the length of a crescent approaches one full turn, macrocyclization through an intramolecular reaction is favored by the preorganization of the molecule. These so-called shape-persistent aromatic amide macrocycles have been thoroughly investigated and exploited for the purpose of molecular recognition.[9] Even when curvature is weak, large macrocycles can be obtained in high yield. In the case of Q oligomers, the preferred curvature is high at 2.5 units per turn. With a small distortion of bending angles, Q can cyclotrimerize into **1.** Its flat structure fulfills local conformational preferences and its inner rim is comparable to a hexa-aza-18-crown-6 with alternating hydrogen-bond donors and acceptors (Figure 1 b,c).[10] A cyclotetramer (**2**) can also be produced under conditions that help destabilize the helical precursor, for example, heat and a high LiI concentration. The cyclotetramer has a saddle-like shape in which two hydrogen bonds are not formed.[10] The formation of such strained structures is both intriguing and informative regarding the hierarchy of forces that stabilize the helical non-cyclic precursors. However, longer helical oligomers than a tetramer cannot be denatured and do not form cycles. We reasoned that introducing removable DMB amide substituents might perturb helical conformations so as to allow macrocyclization. Indeed, aryl-alkyl tertiary amides are known to prefer *cis* conformations.[11] Their use has been

[*] K. Urushibara, Prof. A. Tanatani
Department of Chemistry, Faculty of Science, Ochanomizu University
2-1-1 Otsuka, Bunkyo-ku, Tokyo 112-8610 (Japan)
E-mail: tanatani.aya@ocha.ac.jp
K. Urushibara, Dr. Y. Ferrand, Prof. I. Huc
CBMN (UMR5248), Univ. Bordeaux—CNRS—IPB
Institut Européen de Chimie et Biologie
2 rue Escarpit, 33600 Pessac (France)
Dr. Z. Liu, Prof. V. Pophristic
Department of Chemistry &Biochemistry, University of the Sciences
600 South 43rd Street, Philadelphia, PA 19104 (USA)
Prof. H. Masu
Center for Analytical Instrumentation, Chiba University
1–33 Yayoi, Inage, Chiba 263-8522 (Japan)
Prof. I. Huc
Department Pharmazie, Ludwig-Maximilians-Universität
Butenandtstr. 5–13, 81377 München (Germany)
E-mail: ivan.huc@cup.lmu.de
Supporting information and the ORCID identification number(s) for the author(s) of this article can be found under: https://doi.org/10.1002/anie.201802159.

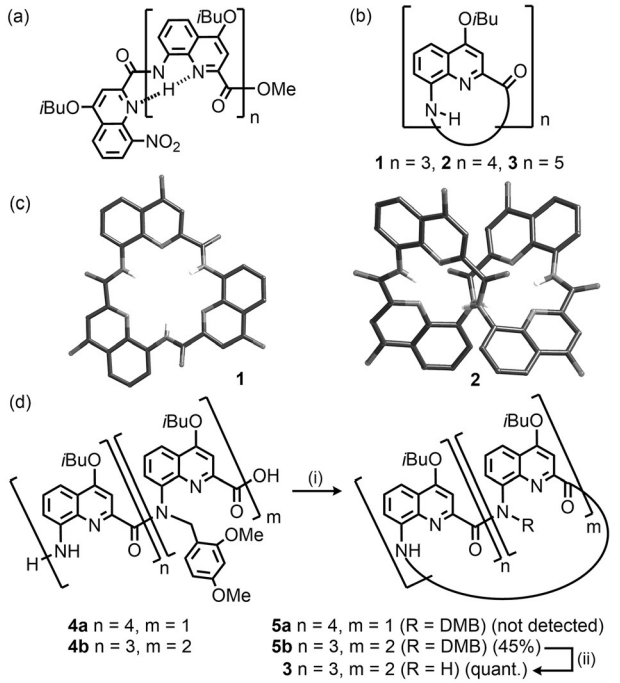

Figure 1. Chemical structures of a) non cyclic 8-amino-2-quinolinecarboxylic acid oligoamides, and b) its macrocycles **1**–**3**. c) Crystal structures of **1** and **2**. d) Macrocyclization of **4**. Conditions: i) PPh_3, trichloroacetonitrile, DIPEA, $CHCl_3$; ii) TFA (neat), 60 °C. DMB = 2,4-dimethoxybenzyl, DIPEA = diisopryopylethlamine, TFA = trifluoroacetic acid.

proposed before to reduce steric hindrance in single helices[12] or to disrupt aggregation in rod-like aromatic amide oligomers.[13] Tertiary amides have also been used as precursors of peptidic macrocycles.[14]

Pentamide amino acid **4a**, which has one tertiary amide bond at its C terminus (Figure 1d), was prepared and submitted to condensation conditions at various temperatures but no macrocycle **5a** was detected. We hypothesized that one tertiary amide bond was insufficient to allow the two ends of the helix to meet and react. Analogue **4b**, which has two consecutive tertiary amide bonds was then prepared (see Scheme S1 in the Supporting Information).[15] By using in situ acid chloride activation with CCl_3CN/PPh_3,[16] **4b** was converted into cyclopentamer **5b** in 45% yield along with seemingly non-cyclic oligomeric byproducts that could not be identified. Removal of the DMB groups using TFA at 60 °C then afforded **3** quantitatively. A systematic investigation of the cyclization yield as a function of the number and position of DMB groups was not carried out. One cannot exclude that a single DMB group at a more central location than in **4a** might also be productive, or that more than two DMB groups might not be beneficial. ROESY and variable-temperature NMR spectra of **4b** showed complex conformational behavior: at least three species coexist under slow exchange, possibly due to *cis*/*trans* isomerism of the tertiary amide bonds (Figures S4, S5). Exchange is slow at temperatures as high as 323 K. Substantial chemical-shift differences between the various species indicated important conformation variations. The complexity of the spectra did not allow a detailed structural investigation. However, the coexistence of multiple species hints at a certain degree of flexibility that could potentially be conducive to cyclization.

The structures of macrocycles **5b** and **3**, as well as of the Fmoc-allyl ester precursor of **4b**, were all elucidated in the solid state by single-crystal X-ray crystallography. Among other features, the precursor of **4b** (Figure 2a) possesses a short helical segment comprised of three quinoline rings and two secondary amides. Its two tertiary amides are *cis*-configured as expected (i.e., the two aryl rings are *cis* to each other). The absence of a hydrogen bond and the bulk associated with the DMB groups bring each tertiary amide out of the plane of its neighbor quinoline rings: aryl amide dihedral angles were measured at 63.2°/63.3° and 82.7°/83.1°, contrary to the secondary amides, which are almost coplanar with adjacent quinoline rings. As a result, the two C-terminal quinoline rings have their planes almost parallel to the helix axis. In this structure, all local conformational preferences are fulfilled. The terminal amine and acid functions are not close to each other or preorganized for cyclization, yet one may expect that the short helical segment may undergo conformational changes at a moderate energy cost.

This hypothesis was confirmed by the crystal structure of cyclopentamide **5b**, which showed that only one (out of three) secondary amides lies in its preferred conformation, that is, almost parallel to neighboring aryl units; the two others are significantly tilted out of plane (aryl-CO dihedral angles at 34.65°/30.62° and aryl-NH dihedral angles at 56.87°/56.38°), thereby allowing one quinoline ring to be almost perpendicular to the two adjacent rings. This conformation is stabilized by an intra-cycle hydrogen bond between one of these amide protons and the carbonyl group of one of the *cis* tertiary amides ($d_{(N\cdots O)} = 2.893$ Å). However, ^{1}H NMR spectra reveal slightly upfield-shifted amide proton signals ($\delta = 11.73, 11.67, 9.71$ ppm) with respect to **4b** ($\delta = 12.65, 11.11$ ppm), which reflects weaker hydrogen bonding (Figure 3a,b). One DMB group is also found stacked face-to-face on a quinoline ring in the crystal structure. Overall, the structure of **5b** is reminiscent of the saddle-shape structure of **2**.[10] These results show that the level of strain required for its formation is not negligible but also that it can be overcome.

The crystal structure of **3** revealed a figure-of-eight flat shape combining two short helix segments with the same handedness. The two segments are connected by two local disruptions of preferred quinoline–amide-linkage conformations. One disruption consists of an entirely flipped quinoline–carbonyl bond (Figure 2c, green), which forces the carbonyl oxygen and endocyclic nitrogen lone pairs to converge despite electrostatic repulsions. This misfolded state was previously calculated as a high-energy intermediate between *P* and *M* helices.[5] The other disruption is a rare *cis* secondary arylamide (Figure 2c, magenta). Thus, the strain associated with the connection of the two diverging ends of a helical pentamide is not distributed across the whole macrocycle but localized at these two points.

The outcome is a markedly different environment for the five units of **3**. Consistently, its NMR spectrum at 263 K is sharp and shows signals spread over a wide range of chemical shifts (Figure 3c). For example, two amide protons resonate

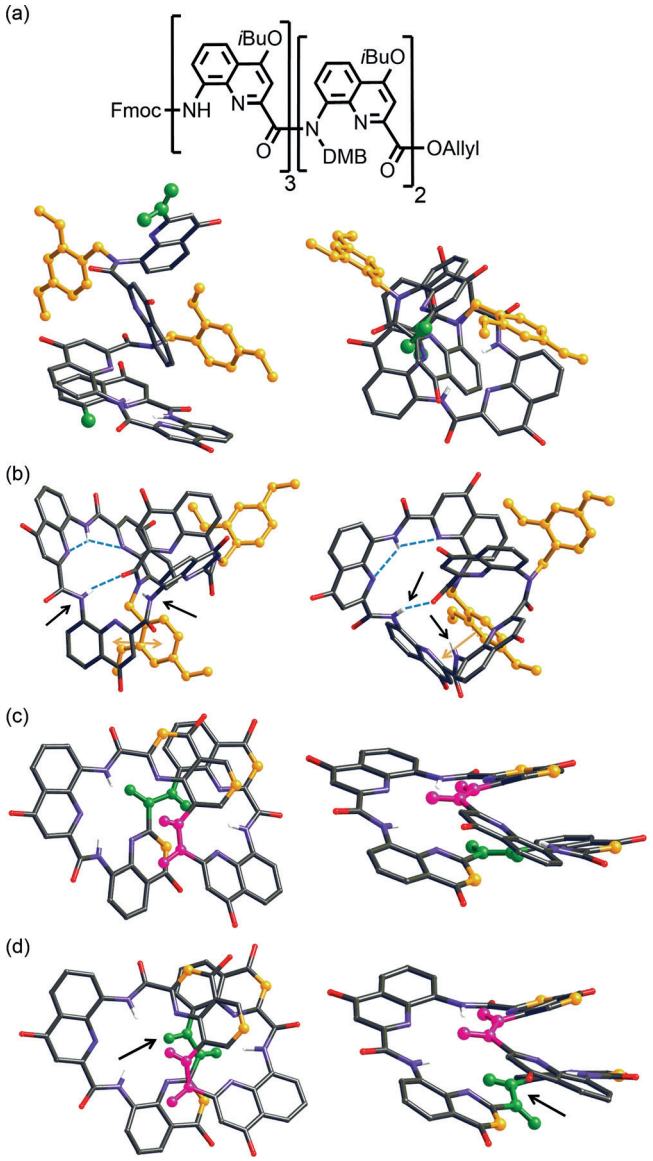

Figure 2. X-ray crystal structures of the different compounds.[23] a) The Fmoc-allyl ester precursor of **4b**. There are two independent molecules with similar conformations in the asymmetric unit but only one is shown. DMB groups are shown as orange ball-and-stick representations. The N-terminal nitrogen atom and C-terminal carboxyl group are shown in green ball-and-stick representation. b) Structure of **5b**. The out-of-plane secondary amides are indicated by arrows. Some intramolecular hydrogen bonds are shown in blue dashed lines. Intramolecular aromatic stacking of a DMB group is marked by a golden double headed arrow. c) Structure of **3**. The *cis* and flipped amide groups are shown as magenta and green ball-and-stick models, respectively. C3 and C6 carbons which bond to upfield shifted H3 and H6 protons are shown as golden balls. d) Snapshot of a higher-energy intermediate found in molecular dynamics simulations of **3**. The color code is the same as in (c). Note that the green amide indicated by arrows is rotated 180° with respect to the most stable structure shown in (c). Hydrogen atoms other than NH, ester and Fmoc groups in (a), isobutoxy side chains, and solvent molecules have been removed for clarity.

upfield at 8.95 and 8.82 ppm due to the loss of hydrogen bonds, one at 10.85 ppm, and two others are found downfield

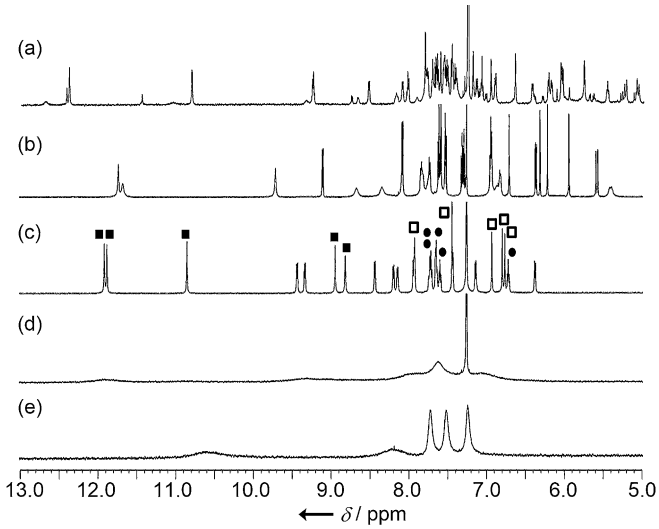

Figure 3. ^{1}H NMR spectra of a) the Fmoc-allyl ester precursor of **4b** at 293 K in $CDCl_3$, b) **5b** at 293 K in $CDCl_3$, c) **3** at 263 K and d) **3** at 313 K in $CDCl_3$, and e) **3** at 373 K in [D_6]DMSO. Amide NH protons and H3 and H6 protons of quinoline rings are marked with filled squares (■), hollow squares (□), and filled circles (●), respectively.

at 11.91 and 11.87 ppm. Similarly, four H6 resonances are clustered near 7.6 ppm, whereas one is found at 6.72 ppm. These were assigned to the four H6 protons lying at the periphery of the macrocycle, and to the H6 proton involved in aromatic stacking in the center of the structure, respectively. Conversely, the signals of the H3 protons span over 1 ppm, with three of them upfield-shifted at 6.94, 6.80 and 6.77 ppm as a consequence of ring-current effects resulting from intramolecular aromatic stacking. Upon cooling to 223 K, the chemical-shift values vary little, thus indicating limited structural variations (Figure S2).

Upon heating a solution of **3** in $CDCl_3$ up to 313 K, the signals broaden, which suggests that some exchange takes place (Figure 3d). In [D_6]DMSO, coalescence occurs at 333 K and the signals sharpen again at 373 K in a simplified spectrum, thus showing that all the rings are equivalent on average. This demonstrates that the points of disruption of helicity circulate along the macrocycle, which thus shows fluxional behavior. Interestingly, the anisochronous signals of the diastereotopic side chain CH_2 protons also coalesce upon heating, thus indicating fast *P*-macrocycle/*M*-macrocycle equilibrium at high temperature (see below).

Macrocycle **3** may in principle form ten degenerate conformers, depending on whether the *cis*-amide bond is connected to position 2 of any of the five quinoline rings, and whether helicity is *P* or *M*; accordingly, these conformers can be termed P_1–P_5 and M_1–M_5.[17] Four mechanisms of exchange between the conformers can be then envisaged, two with retention of chirality, two with inversion of chirality: $P_i <=> P_{i+1}$, $P_i <=> M_{i+1}$, $P_i <=> P_{i+2}$, and $P_i <=> M_{i+2}$. Other trajectories involving $i-1$, $i-2$, $i \pm 3$, or $i \pm 4$ are redundant with these four. In addition, non-fluxional inversion of handedness ($P_i <=> M_i$) may be considered. We used molecular dynamics simulations to assess whether any of these mechanisms prevail. Specifically, we generated trajectories

amounting to 10 μs through either simulated annealing, that is, heating–cooling cycles between 300 K and 800 K, or through metadynamics simulations[5,18] using different sets of collective variables, in the presence (as in **3**) or absence of isobutoxy side chains. The results (see the Supporting Information for details) confirm the prevalence of the crystal structure as a unique degenerate energy minimum in which the amide in position 2 of unit *i* is *cis*, and the *trans* amide in position 2 of unit $i+3$ is singly instead of doubly hydrogen bonded due to a flipped quinoline–carbonyl bond. They also reveal the existence of a higher-energy local minimum in which the amide in position 2 of unit $i+3$ is flipped by 180° (Figure 2d). This local minimum is a frequent intermediate during the exchange between degenerate lower-energy conformers, which are found to occur via two privileged pathways. Out of 99 exchange trajectories, 52 are of the kind $P_i <=> P_{i+2}$ and 42 of the kind $P_i <=> M_{i+1}$. If one considers only the 48 trajectories for macrocycle **3** with side chains, 19 are $P_i <=> P_{i+2}$ and 28 $P_i <=> M_{i+1}$.

The structure and behavior of **3** are related to a few known fluxional macrocycles[19–21] or eight-shaped molecules,[21,22] derived from metal complexes[20] or from expanded porphyrins.[21,22] It contrasts with most aromatic oligoamide macrocycles, which form shaped-persistent planar structures fulfilling the preferred local conformations that promote helical folding in non-cyclic molecules.[9] The uniqueness of **3** stems from its high strain. It derives from a non-cyclic pentamer that would not cyclize if disruptors of helicity had not been transiently introduced. The combination of conformationally very stable short helix segments and two high-energy conformations, in particular a secondary *cis* amide, results in slow dynamics and in defined fluxional pathways. Larger quinolinecarboxamide macrocycles may also be expected to adopt intriguing structures while striving to maximize their helical content despite being constrained in a ring. It remains to be seen whether they would also be fluxional and exchange through well-defined conformational pathways.

Acknowledgements

This work was partly supported by JSPS KAKENHI Grant No 16K08318 (to A.T.) and 17J00036 (to K.U.). A.T. gratefully acknowledges funding from The Sumitomo Foundation and The Naito Foundation. Computational work was supported by NSF grant MRI CHE-1229564. We thank Dr. B. Kauffmann for assistance of X-ray crystallographic analysis.

Conflict of interest

The authors declare no conflict of interest.

Keywords: *cis* amides · fluxionality · frustrated helicity · macrocycles · strained structures

How to cite: *Angew. Chem. Int. Ed.* **2018**, *57*, 7888–7892
Angew. Chem. **2018**, *130*, 8014–8018

[1] T. C. Boles, J. H. White, N. R. Cozzarelli, *J. Mol. Biol.* **1990**, *213*, 931.
[2] M. Szostak, J. Aubé, *Chem. Rev.* **2013**, *113*, 5701; M. Liniger, D. G. VanderVelde, M. K. Takase, M. Shahgholi, B. M. Stoltz, *J. Am. Chem. Soc.* **2016**, *138*, 969.
[3] J. Clayden, A. Lund, L. Vallverdú, M. Helliwell, *Nature* **2004**, *431*, 966.
[4] J. Zhang, M. W. Germann, *Biopolymers* **2011**, *95*, 755; A. Jabs, M. S. Weiss, R. Hilgenfeld, *J. Mol. Biol.* **1999**, *286*, 291; D. E. Stewart, A. Sarkar, J. E. Wampler, *J. Mol. Biol.* **1990**, *214*, 253; M. S. Weiss, A. Jabs, R. Hilgenfeld, *Nat. Struct. Biol.* **1998**, *5*, 676; M. W. MacArthur, J. M. Thornton, *J. Mol. Biol.* **1991**, *218*, 397.
[5] A. M. Abramyan, Z. Liu, V. Pophristic, *Chem. Commun.* **2016**, *52*, 669.
[6] I. Huc, *Eur. J. Org. Chem.* **2004**, 17; D.-W. Zhang, X. Zhao, J.-L. Hou, Z.-T. Li, *Chem. Rev.* **2012**, *112*, 5271; L. Yuan, H. Zeng, K. Yamato, A. R. Sanford, W. Feng, H. S. Atreya, D. K. Sukumaran, T. Szyperski, B. Gong, *J. Am. Chem. Soc.* **2004**, *126*, 16528; L.-Y. You, S.-G. Chen, X. Zhao, Y. Liu, W.-X. Lan, Y. Zhang, H.-J. Lu, C.-Y. Cao, Z.-T. Li, *Angew. Chem. Int. Ed.* **2012**, *51*, 1657; *Angew. Chem.* **2012**, *124*, 1689.
[7] H. Jiang, J.-M. Léger, I. Huc, *J. Am. Chem. Soc.* **2003**, *125*, 3448; N. Delsuc, T. Kawanami, J. Lefeuvre, A. Shundo, H. Ihara, M. Takafuji, I. Huc, *ChemPhysChem* **2008**, *9*, 1882; T. Qi, V. Maurizot, H. Noguchi, T. Charoenraks, B. Kauffmann, M. Takafuji, H. Ihara, I. Huc, *Chem. Commun.* **2012**, *48*, 6337; S. J. Dawson, Á. Mészáros, L. Pethö, C. Colombo, M. Csékei, A. Kotschy, I. Huc, *Eur. J. Org. Chem.* **2014**, 4265.
[8] J. Zhu, R. D. Parra, H. Zeng, E. Skrzypczak-Jankun, X. C. Zeng, B. Gong, *J. Am. Chem. Soc.* **2000**, *122*, 4219.
[9] X. Ki, X. Yuan, P. Deng, L. Chen, Y. Ren, C. Wang, L. Wu, W. Feng, B. Gong, L. Yuan, *Chem. Sci.* **2017**, *8*, 2091; X. Li, B. Li, L. Chen, J. Hu, C. Wen, Q. Zheng, L. Wu, H. Zeng, B. Gong, L. Yuan, *Angew. Chem. Int. Ed.* **2015**, *54*, 11147; *Angew. Chem.* **2015**, *127*, 11299; Y. Yang, W. Feng, J. Hu, S. Zou, R. Gao, K. Yamato, M. Kline, Z. Cai, Y. Gao, Y. Wang, Y. Li, Y. Yang, L. Yuan, X. C. Zeng, B. Gong, *J. Am. Chem. Soc.* **2011**, *133*, 18590; Y. Liu, J. Shen, C. Sun, C. Ren, H. Zeng, *J. Am. Chem. Soc.* **2015**, *137*, 12055; B. Qin, C. Ren, R. Ye, C. Sun, K. Chiad, X. Chen, Z. Li, F. Xue, H. Su, G. A. Chass, H. Zeng, *J. Am. Chem. Soc.* **2010**, *132*, 9564; B. Qin, X. Chen, X. Fang, Y. Shu, Y. K. Yip, Y. Yan, S. Pan, W. Q. Ong, C. Ren, H. Su, H. Zeng, *Org. Lett.* **2008**, *10*, 5127; Y.-Y. Zhu, C. Li, G.-Y. Li, X.-K. Jiang, Z.-T. Li, *J. Org. Chem.* **2008**, *73*, 1745.
[10] H. Jiang, J.-M. Léger, P. Guionneau, I. Huc, *Org. Lett.* **2004**, *6*, 2985.
[11] A. Itai, Y. Toriumi, N. Tomioka, H. Kagechika, I. Azumaya, K. Shudo, *Tetrahedron Lett.* **1989**, *30*, 6177; A. Itai, Y. Toriumi, S. Saito, H. Kagechika, K. Shudo, *J. Am. Chem. Soc.* **1992**, *114*, 10649; A. Tanatani, I. Azumaya, H. Kagechika, *J. Synth. Org. Chem. Jpn.* **2000**, *58*, 556.
[12] A. Zhang, J. S. Ferguson, K. Yamato, C. Zheng, B. Gong, *Org. Lett.* **2006**, *8*, 5117.
[13] H. M. König, T. Gorelik, U. Kolb, A. F. M. Kilbinger, *J. Am. Chem. Soc.* **2007**, *129*, 704.
[14] W. D. F. Meutermans, G. T. Bourne, S. W. Golding, D. A. Horton, M. R. Campitelli, D. Craik, M. Scanlon, M. L. Smythe, *Org. Lett.* **2003**, *5*, 2711; K. J. Jensen, J. Alsina, M. F. Songster, J. Vágner, F. Albericio, G. Barany, *J. Am. Chem. Soc.* **1998**, *120*, 5441.
[15] T. Qi, T. Deschrijver, I. Huc, *Nat. Protoc.* **2013**, *8*, 693.
[16] G.-C. Wu, H. Tanaka, K. Sanui, N. Ogata, *Polym. J.* **1982**, *14*, 797; X. Hu, S. J. Dawson, Y. Nagaoka, A. Tanatani, I. Huc, *J. Org. Chem.* **2016**, *81*, 1137; M. L. Singleton, G. Pirotte, B. Kauffmann, Y. Ferrand, I. Huc, *Angew. Chem. Int. Ed.* **2014**, *53*, 13140; *Angew. Chem.* **2014**, *126*, 13356.

[17] Numbering nomenclature is as in peptides: the carbonyl of unit *i* is attached to the amine of unit $i+1$.
[18] A. Laio, M. Parrinello, *Proc. Natl. Acad. Sci. USA* **2002**, *99*, 12562; Z. Liu, X. Hu, A. M. Abramyan, Á. Mészáros, M. Csékei, A. Kotschy, I. Huc, V. Pophristic, *Chem. Eur. J.* **2017**, *23*, 3605.
[19] Y. Chen, D.-X. Wang, Z.-T. Huang, M.-X. Wang, *J. Org. Chem.* **2010**, *75*, 3786; L.-X. Wang, D.-X. Wang, Z.-T. Huang, M.-X. Wang, *J. Org. Chem.* **2010**, *75*, 741; M. Yoshikawa, S. Imigi, K. Wakamatsu, T. Iwanaga, S. Toyota, *Chem. Lett.* **2013**, *42*, 559; M. Inoue, T. Iwanaga, S. Toyota, *Bull. Chem. Soc. Jpn.* **2015**, *88*, 1591.
[20] T. Gyr, H. R. Mäck, M. Hennig, *Angew. Chem. Int. Ed. Engl.* **1997**, *36*, 2786; *Angew. Chem.* **1997**, *109*, 2869.
[21] N. Sprutta, L. Latos-Grażyński, *Chem. Eur. J.* **2001**, *7*, 5099; H. Maeda, T. Nishimura, R. Akuta, K. Takaishi, M. Uchiyama, A. Muranaka, *Chem. Sci.* **2013**, *4*, 1204.
[22] A. Ghosh, A. Srinivasan, C. H. Suresh, T. K. Chandrashekar, *Chem. Eur. J.* **2016**, *22*, 11152; J. Setsune, *J. Chem. Sci.* **2012**, *124*, 1151; T. Y. Gopalakrishna, V. G. Anand, *Angew. Chem. Int. Ed.* **2014**, *53*, 6678; *Angew. Chem.* **2014**, *126*, 6796; T. Yoneda, S. Saito, H. Yorimitsu, A. Osuka, *Angew. Chem. Int. Ed.* **2011**, *50*, 3475; *Angew. Chem.* **2011**, *123*, 3537; K. Moriya, S. Saito, A. Osuka, *Angew. Chem. Int. Ed.* **2010**, *49*, 4297; *Angew. Chem.* **2010**, *122*, 4393; C. Bucher, D. Seidel, V. Lynch, J. L. Sessler, *Chem. Commun.* **2002**, 328; R. Misra, T. K. Chandrashekar, *Acc. Chem. Res.* **2008**, *41*, 265; Z. Zhang, W.-Y. Cha, N. J. Williams, E. L. Rush, M. Ishida, V. M. Lynch, D. Kim, J. L. Sessler, *J. Am. Chem. Soc.* **2014**, *136*, 7591.
[23] CCDC 1824124 (**18**), 1585727 (**5b**), and 1585728 (**3**) contain the supplementary crystallographic data for this paper. These data can be obtained free of charge from The Cambridge Crystallographic Data Centre.

Manuscript received: February 17, 2018
Accepted manuscript online: April 14, 2018
Version of record online: May 16, 2018

